A Systematic Study to Unravel the Potential of using Polysaccharides based Organic Nanoparticles Versus Hybrid Nanoparticles for Pesticide Delivery

Ritu Mahajan,† Abdul Selim,† K. M. Neethu, Sandeep Sharma, Vijayakumar Shanmugam, Govindasamy Jayamurugan*

Institute of Nano Science and Technology, Knowledge City, Sector 81, SAS Nagar, Manauli PO, Mohali, Punjab 140306, India.

† Authors contributed equally

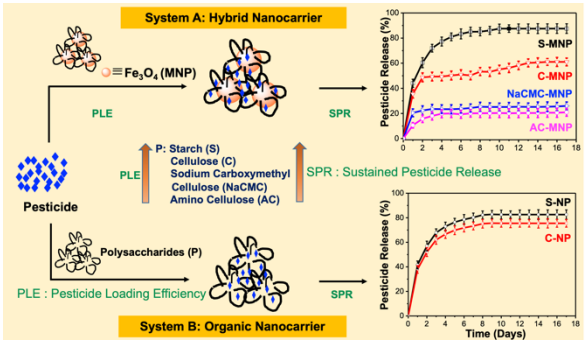

ABSTRACT: To daze conventional pesticide release limitations, nanotechnology-mediated pesticide delivery using natural polymers has been actively investigated. However, the lack of information on what are the beneficial/non-beneficial aspects of using hybrid- and organic-nanoparticles (NP) and among the polysaccharides which are better suited concerning pesticide loading efficiency (PLE wt%), entrapment efficiency (E.E %), and sustained-pesticide-release (SPR %) has prompted us to investigate this study. In this report, we systematically investigated a series of polysaccharides such as starch (S), cellulose (C), aminocellulose (AC), and sodium carboxymethylcellulose (NaCMC) coated on magnetite NP (MNP, Fe_3O_4) and complete organic nanocarrier systems (starch and cellulose) that have no MNP part were compared for the PLE wt% and SPR % efficiencies for chlorpyrifos (ChP) insecticide. Overall, all nanocarriers (NCs) have shown good to excellent PLE wt% due to the smaller-sized NP obtained through optimal conditions. However, among the hybrid polysaccharides studied, starch MNP (S-MNP) has shown a maximum PLE of 111 wt% in comparison with other polysaccharides (80 – 94 wt%) coated hybrid-NCs as well as with organic-NCs (81 – 87 wt%). The use of inorganic support does improve the PLE wt% markedly for starch but not for

cellulose derivatives. Similarly, the SPR results of S-NP showed a remarkably better sustained-release profile for ChP of 88 % in 14 days. In contrast, other unfunctionalized and functionalized celluloses exhibited poor release profiles of 60 – 20 % for the same period. This study may help the researchers choose the right system for designing and achieving enhanced pesticide efficiency.

KEYWORDS: Pesticide; Polysaccharides; nanoencapsulation; iron oxide nanoparticles; sustained release; chlorpyrifos.

1. INTRODUCTION

To serve food for an increasing population worldwide, there is a tremendous need to ensure the sustainability of food.[1] Pesticide plays an inextricable role in improving crop protection, thereby securing food security for the global population.[2,3] Meticulous pesticide release schemes are cast off on farmlands by picking an appropriate and judicious administration course to control the target pest accurately.[4,5] In the last decade, the application of nanomaterials in the arena of pesticides has made significant strides.[6-12] This knowledge aims to lessen the unperceptive usage of conventional pesticides and safeguard their innocuous submission.[13] In particular, nanomaterials with targeted and controlled release properties can expand the pesticide application and lessen residue and contamination.[10,14-19] The prime benefit of measured-release preparation is that they let considerably fewer pesticides be used for the same period of action. Furthermore, unlike conventional pesticide delivery, the use of nanocarrier can enhance the efficacy and protect the pesticide, which is beneficial, especially when pesticide with short-lifetime is to be used.[20]

Diverse materials such as metal oxides,[21-23] SiO_2,[24-28] graphene derivatives,[29-31] polymers,[32-35] polysaccharides,[36-38] nanocomposites,[39] etc. have been cast-off for the controlled release of pesticides. Among these systems, natural biodegradable polymers have been extensively studied for agricultural applications[20,40] besides drug delivery,[34,38,41-43] tissue engineering,[34,43-45] cosmetics,[46] and food,[20,37,47-51] etc. In particular, polysaccharides and their nanocomposites with metal oxides are considered a good nanocarrier for pesticide delivery due to their characteristic features such as natural abundance, biocompatibility, easy functionalization etc (Figure 1).[4,5,22,36,37] Unlike drug therapy, the agriculture sector demands sustainable drug release over an extended period, which is a critical parameter apart from PLE wt%. So far, the polysaccharides namely alginate/starch/clay,[52] alginates/bentonite,[53-55] alginate/chitosan,[56] hydrogels of calcium and nickel alginates,[57] starch/gaur-gum,[58] ethylcellulose,[59-61]

ethylcellulose-lignin,[62] polysaccharides-clay nanocomposites,[63-64] and macro to micro-sized spheres/beads obtained with various crosslinking agents[65-66] were primarily used as insecticide carrier. Though many reports were dealt with the macro- to micro-particles,[21,47] it has been shown that particle size reduction to nano-size exhibited pronounced E.E % and SPR % values due to more rooms (surface area) available for insecticide molecules to get entrapped. However, in general, the existing polysaccharides based nanocarriers have shown fast pesticide release (8 h to 6 days), presumably due to the sub-micron size of the particles (100–800 nm) (Table S4, Supporting Information (SI)).

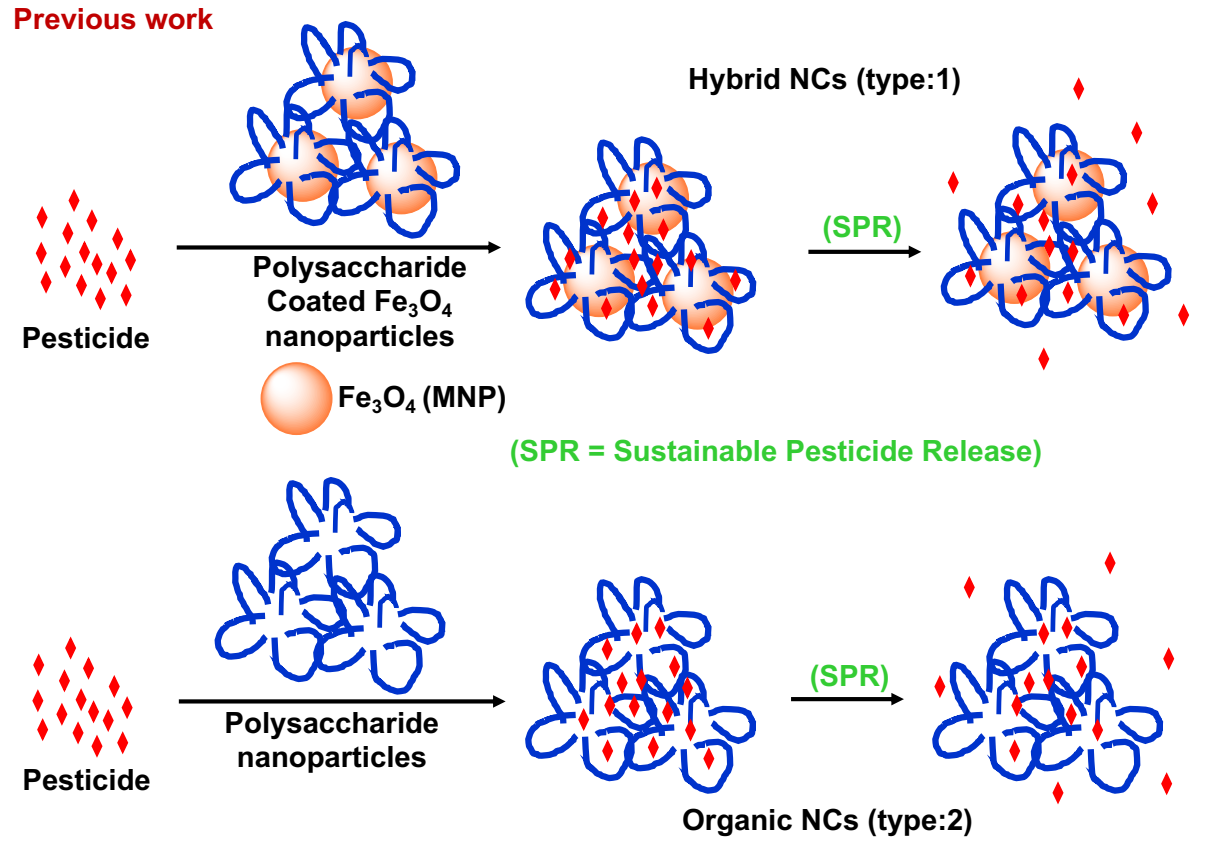

Figure 1. Schematic representation of two types of systems evaluated for pesticide loading and release profile.

Nevertheless, the above examples infer that carbohydrates are promising candidates and still offer more rooms to improve the PLE wt% and SPR % properties combined with nanotechnology. Thus, to achieve upright sustained pesticide release and enhanced PLE wt%, we synthesized a series of even smaller sized NP of polysaccharides (cellulose, functionalized cellulose, and starch) without and in combination with iron oxide NP (MNP, Fe_2O_3) as hybrid particles by tweaking the weak acid sonication, nanoprecipitation and co-precipitation methods

respectively (Scheme 1). Another primary objective of this study is to find that which polysaccharide is better suited for organic *vs* hybrid pesticide nanocarrier. This is the first systematic relative account of E.E %, PLE wt%, and aqueous release behavior of chlorpyrifos (ChP) from organic versus hybrid nanomaterials (Figure 1).

2. EXPERIMENTAL SECTION

2.1 Materials and Reagents. Iron (III) chloride hexahydrate ($FeCl_3.6H_2O$); iron (II) chloride tetrahydrate ($FeCl_2.4H_2O$); microcrystalline cellulose $(C_6H_{10}O_5)_n$, urea, chlorpyrifos, and ethylenediamine were obtained from Sigma-Aldrich. Sodium carboxymethylcellulose, starch, hydrochloric acid (HCl), dimethyl sulfoxide (DMSO), sulphuric acid (H_2SO_4), sodium hydroxide (NaOH), perchloric acid ($HClO_4$), isopropanol (*i*PrOH), methanol (MeOH), and acetone (Me_2CO) were obtained from Rankem. Dialysis tubes (MWCO 1KDa) were procured from G-Biosciences. Aminocellulose was synthesized from microcrystalline cellulose as per the literature procedure.[67]

2.2 Characterization Methods. X-ray Diffraction (XRD) was performed using Bruker D-8 advanced diffractometer in the 2θ range of 10 to 90 degree. The average crystalline size of NP with and without surface coating was estimated using the Scherrer equation. Fourier transform infrared (FT–IR) spectra were recorded on Agilent Cary 660 spectrometer using the KBr pellet technique in a range of 4000–400 cm^{-1}. Thermogravimetric analysis (TGA) was performed to determine the degradation/decomposition behavior of samples using thermogravimetric (TG) analyzer-(Perkin Elmer STA 8000) at a N_2 flow rate of 10 mL/min and heating rate of 10 °C/min. Magnetic measurements of MNP, C-MNP, NaCMC-MNP, AC-MNP, and S-MNP were performed using Dynacool, 14 T physical property measurement system (PPMS) at room temperature, with a magnetic field in the range of –15000 to 15000 Oe, and parameters such as saturation magnetization (M_{sat}), and coercive field (Hc) were evaluated. Atomic force microscopy (AFM) images were acquired using NanoScope 9.1, Bruker Multimode 8 in a tapping mode. The samples were deposited on silicon wafers and analysis was performed at different sections at room temperature and ambient atmosphere. Transmission electron microscopy (TEM) images were acquired on a JEOL-JSM2100 HR operating at 200 kV. Samples were prepared by depositing a drop of diluted NP suspension on 300 mesh TEM grid followed by dried under vacuum for 24 h. Scanning electron microscopy (SEM) images were acquired on a (JEOL, JSM-IT300). Inductively coupled plasma-mass spectrometer (ICP-MS, Model: Agilent 7700 Series provided by Punjab Biotechnology Incubator, Mohali, India), the analysis was performed to estimate the percentage of iron oxide content in the hybrid-NCs.

The GC-MS analysis was performed to determine the E.E% and PLE wt% using a Shimadzu GC coupled with a GCMS-QP 2010 plus mass detector and a single-quadrupole mass spectrometer Quantum (Shimadzu) with 100% dimethyl polysiloxane (Restek Rxi-1ms; 30 m × 0.25 mmiD., 0.25 μm film thickness) column. GC-MS operating conditions: The initial oven temperature was 60 °C, maintained for 1 min and then ramped to 270 °C at a rate of 10 °C/min followed by holding for 5 min at 270 °C. The initial temperature of the injector was 63 °C and then programmed at the same rate as the oven. Helium was used as carrier gas with primary pressure of 570 KPa. The split injection mode was used with a split ratio of 10.0. The injection volume of each sample was 1 μL and the total time for one GC-MS run was 27 min. Mass spectrometer settings: electron impact ionization mode with an electron energy of 70 eV, ion source and interface temperatures were set at 200 and 270 °C, respectively and scan mass range *m/z* 50–500. Shimadzu 2600 UV-Vis spectrophotometer was used to estimate the amount of entrapped pesticide at 290 nm during the aqueous release study after every 24 h. The calibration curve of ChP was prepared in MeOH. The pesticide release rates were analyzed by applying different models such as Korsmeyer–Peppas,[68a] Peppas–Sahlin[68b] and Makoid–Banakar[69] with DD solver software, which is the Excel-plugin module to understand the release kinetics mechanism of the entrapped ChP molecules from the NCs.

2.3 Synthesis of hybrid- and organic-nanoparticles as pesticide nanocarriers (NCs). In this study, two types of nanocarriers i.e. hybrid and organic have been designed and synthesized (Scheme 1). Hybrid-NCs such as C-MNP, AC-MNP,[67] NaCMC-MNP and S-MNP comprising of magnetite nanoparticles (MNP) coated with various polysaccharides such as cellulose (C), aminocellulose (AC), sodium carboxymethylcellulose (NaCMC), and starch (S) were synthesized (Scheme 1a). These polysaccharides have been used as stabilizers or capping agents for the *in situ* prepared smaller-sized superparamagnetic iron oxide nanoparticles (SPIONS).

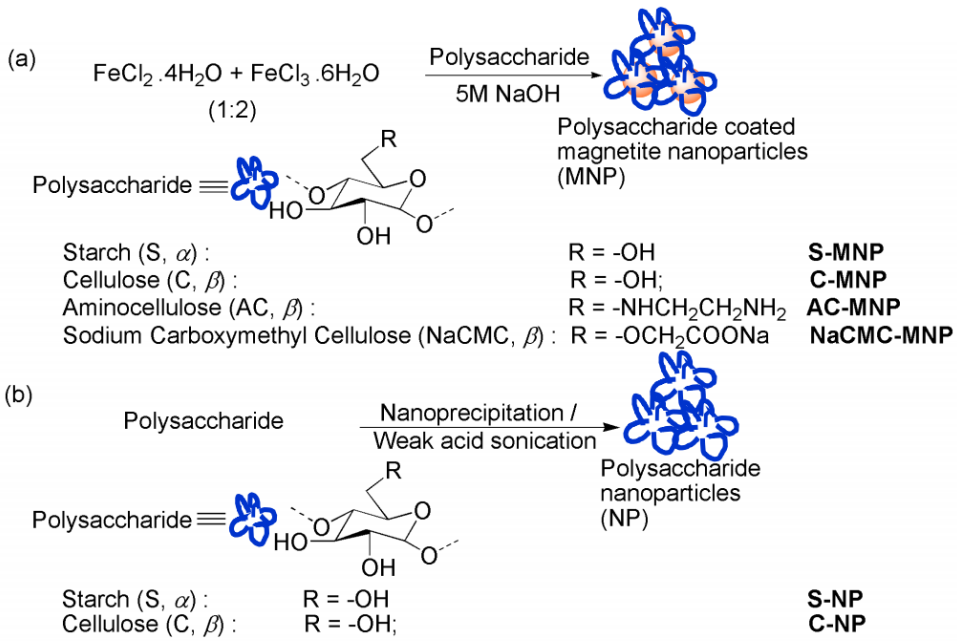

Scheme 1. Synthesis of a) hybrid-NCs based on polysaccharide coated magnetite NP, b) organic-NCs based on polysaccharide NP.

2.3.1 General procedure for hybrid-NCs (S-MNP, C-MNP, AC-MNP, NaCMC-MNP). The procedure for the synthesis of hybrid-NCs was adopted from the literature with slight modification.[22] Magnetite NP (Fe_3O_4, MNP) were prepared by the co-precipitation method. Iron dichloride tetrahydrate ($FeCl_2 \cdot 4H_2O$, 7.3 g, 0.037 mol) and iron trichloride hexahydrate ($FeCl_3 \cdot 6H_2O$, 5 g, 0.0185 mol) were mixed in 100 mL of 2 M HCl at 40 °C. The blend was released into polysaccharides (5 g in 60 mL of water) and 100 mL of 2M NaOH solution under vigorous stirring for about 30 min. The resulting solution was stirred (200 rotations per minute (rpm)) and heated at 90 °C for 1 h. The 5 M NaOH was added dropwise to obtain a pH of 11. The precipitate was centrifuged and treated repeatedly with 3 M $HClO_4$ solution to bring a pH of 3. After the last separation by centrifugation, the particles were dispersed into polysaccharides (5 g in 60 mL of water). The polysaccharide-coated iron oxide nanocomposites were obtained by centrifugation followed by drying the material at 40 °C to give the corresponding hybrid-NCs (Scheme 1a).

2.3.2 Synthesis of organic-NCs (C-NP, S-NP). In the case of organic-NCs, the cellulose- and starch-nanoparticles were prepared by the nanoprecipitation method in the absence of MNP.

(i) Preparation of cellulose nanoparticles (C-NP). The procedure for the synthesis of C-NP was adopted from the literature with slight modification (Scheme 1b).[70] Microcrystalline cellulose (5 g) was dispersed into 40 mL of the alkaline solution (5 M NaOH) made with cold

deionized (DI) water and heated to 80 °C for 3 h. Then the slurry was filtered and thoroughly washed with DI water until the wash water is neutral pH. The resulting residue was air-dried and then transferred into DMSO (40 mL) followed by heating to 80 °C for 3 h. The solution was then filtered and washed with DI water (3 × 20 mL). The pretreated fibers were transferred into 170 mL of an aqueous acidic solution (made of 120 mL DI water, 20 mL 12.1 N HCl, and 60 mL 36 N H_2SO_4). This suspension was sonicated at 80 °C for 8 h. In this hydrolysis process, the fiber slurry solution has turned into milky colloid suspension. This suspension was then centrifuged at 2000 rpm and washed continuously with the addition of DI water (3 × 20 mL). After washing, 2 N NaOH was added to adjust the solution to pH 7. The neutralized products were further washed with (3 × 20 mL) DI water. The residue obtained after the dialysis was freeze-dried and stored at 5 °C for further process.

(ii) Preparation of starch nanoparticles (S-NP). The procedure for synthesizing S-NP was adopted from the literature with slight modification (Scheme 1b).[71] Starch (5 g) was dispersed in 50 mL of the alkaline/urea solution (NaOH (0.8 wt%, 200 mg in 25 mL) and urea (1 wt%, 250 mg in 25 mL) were dissolved in cold deionized water) and heated to 68 °C for 15 h. Then the solution was cooled to 25 °C and filtered. The filtered starch solution was added dropwise at a rate of 1 mL/min with a syringe into 200 mL of ethanol, stirring at 350 rpm. The starch nanoparticles suspension was centrifuged at 8000 rpm for 10 min and washed twice with ethanol (3 × 20 mL). Then the obtained starch nanoparticles (S-NP) were re-dispersed into DI water to get the dispersed solution and for dry powder. The solution was frozen at –80 °C and freeze-dried for various measurements.

2.3.3 General procedure for loading ChP into hybrid and organic-NCs (C-MNP/AC-MNP/NaCMC-MNP/S-MNP) and organic-NCs (C-NP/S-NP). A methanolic (2 mL) solution of ChP (20 mg) was added dropwise to a suspension of hybrid-NC (S-MNP/C-MNP/AC-MNP/NaCMC-MNP, 90 mg) or organic-NC (S-NP/C-NP, 90 mg) in MeOH (10 mL) and stirred at 500 rpm for 3 h at 25 °C (Figure 2). The ChP loaded nanocarriers (ChP-NCs) were collected with the help of an external magnet, washed with methanol, and vacuum dried at 37 °C for 1 h. The supernatant was collected to estimate EE % and PLE wt%.

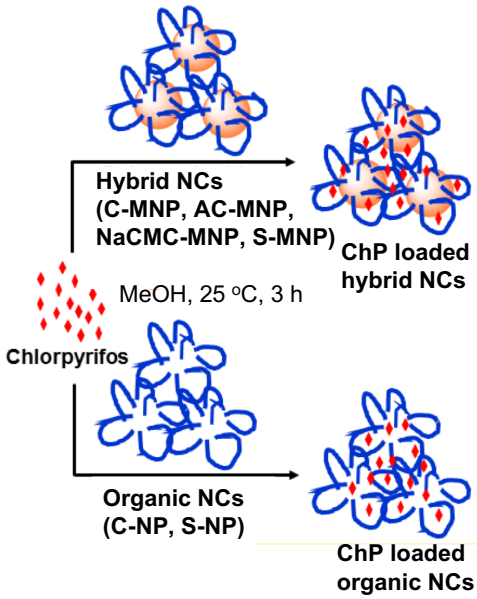

Figure 2. Synthesis of ChP loaded NCs.

2.4 Quantification of pesticide loading efficiency (PLE wt%) and entrapment efficiency (E.E %). The amount of free pesticide present in the supernatant was calculated using gas chromatography−mass spectrometry (GC–MS) analysis with a retention time of 19.9 min (Section B in the SI). The calibration curve of ChP was prepared in MeOH (Figure S8, SI). PLE (wt%) and E.E% were calculated using the following equations and the data are provided in Tables S2 and S3, SI.

$$\text{E. E\%} = \frac{\text{Amount of pesticide} - \text{Amount of free pesticide}}{\text{Total amount of pesticide}} \times 100 \qquad (1)$$

$$\text{PLE wt\%} = \frac{\text{Amount of pesticide} - \text{Amount of free pesticide}}{\text{Total amount of particles}} \times 100 \qquad (2)$$

2.4.1 The PLE wt% and E.E % values correction by ICP–MS for hybrid-NCs. Since the pesticide loading and entrapment occurs only in the organic part of hybrid NCs, i.e., the polysaccharide layer, for a fair comparison, the wt% and E.E % should be compared with a similar amount of organic content present in the NCs. Since the pesticide loading study was carried out with the same amount (90 mg) for both the hybrid and organic NCs, the results were corrected by substituting the percentage of inorganic content present in the hybrid-NCs. The percentage of iron oxide content in the hybrid-NCs such as C-MNP, AC-MNP, NaCMC-MNP, and S-MNP was estimated as 12.27, 8.04, 19.06, and 15.73%, respectively, by using the ICP-MS (GC-MS/ ICP-MS data available in Section B, SI).

2.5 Aqueous release behavior of ChP from hybrid- and organic-NCs. *In vitro,* aqueous release profiles of the ChP in various NCs were carried out by adding 110 mg of the dried ChP

loaded NCs of each formulation in water (10 mL) and stirred at 25 °C. The UV–Vis spectrophotometer was used to analyze the time-dependent release of the ChP from their nano-formulations in water every 24 h up to 17 days. All the experiments were carried out in triplicate.

3. RESULTS AND DISCUSSION

3.1. Synthesis of hybrid- and organic-nanoparticles as pesticide nanocarriers (NC). In this study, we have chosen polysaccharides such as cellulose (C), aminocellulose (AC), sodium carboxymethylcellulose (NaCMC), and starch (S) because cellulose and starch are the least studied polysaccharides in the field of pesticide delivery in comparison with chitosan and alginate (Table S4, SI).[14,37,47] In addition, cellulose and starch are the most abundant natural polymers (biomass) on earth, which is complimentary for agricultural applications. For the inorganic part, we chose SPIONS of magnetite nanoparticle (MNP) (iron oxide, Fe_3O_4) because it has been widely used for pesticide delivery application due to its characteristic features like low-cost and superparamagnetic property.

3.1.1 Synthesis of hybrid-nanoparticles. As shown in Figure 2, the polysaccharides (C/NaCMC, and S) required to synthesize hybrid-NCs such as C-MNP, NaCMC-MNP, and S-MNP were purchased commercially. While synthesis and characterization of aminocellulose,[67a] has been recently reported by our group. In-situ generation of MNP[67] and stabilization by corresponding polysaccharides lead to the isolation of hybrid-NCs such as C-MNP, AC-MNP, NaCMC-MNP, and S-MNP in substantial conversion. Due to the presence of poly hydroxyl groups, the polysaccharides act as templates for the development of nanosized Fe_3O_4 as they impart dynamic supramolecular associations facilitated by inter- and intra-molecular hydrogen bonding interactions. All the synthesized nanocomposites were dense with a smooth surface and easy to handle when dried off (Scheme 1).

3.1.2 Synthesis of organic-nanoparticles. In order to understand the importance of having SPIONS in the hybrid-NCs, we have synthesized organic-NCs from cellulose and starch independently to provide C-NP[70] and S-NP[71], respectively. The syntheses of these organic NP were achieved using week-acid sonication and nanoprecipitation methods, respectively as reported with slight modifications.

3.2 Characterization of hybrid- and organic-nanoparticles. Characterization of organic-NCs (C-NP and S-NP) and hybrid nanocomposites (C-MNP, AC-MNP, NaCMC-MNP, and S-MNP) were investigated by FT–IR, PXRD, TEM, AFM, and TGA analysis. The ICP–MS and

magnetometry analysis was also carried out on hybrid nanocomposites to quantify the iron oxide content and magnetization property, respectively. The details are discussed below.

3.2.1 FT–IR analysis. Comparative FT–IR spectra of hybrid- and organic-NCs were shown in Figures 3a and 3b, respectively. The bare MNP has shown the characteristic stretching frequencies peak at 605 cm^{-1} for the Fe–O bonds.[67a] All nanocomposites have shown peak at 605 cm^{-1} as well as characteristic peaks of C–H and O–H stretching vibrations at 2900 and 3424 cm^{-1}, respectively, suggesting iron oxide has been synthesized with polysaccharide-coated NCs. However, NaCMC has shown a slight shift in the peak, probably due to COO^- binding on the iron oxide surface, unlike OH binding on the other polysaccharides. The peaks in the spectral range of 900–1500 cm^{-1} were due to ν(C–C) and ν(C–O) stretching vibration with contributions from δ(C–O–H) motion.[22] These results indicate that polysaccharides have clearly attached to the surface of the MNP. Similarly, Figure 3b shows the characteristic peaks of O–H stretching vibrations at 3411cm^{-1} and 3416 cm^{-1} for starch and cellulose nanoparticles, respectively. The other characteristic peaks of C–H were observed at wavenumbers of around 2909 cm^{-1} and 2931 cm^{-1} for starch and cellulose nanoparticles, respectively. Moreover, FT–IR spectra also reveal the crystallinity and amorphous domains present inside the starch granules as evidenced from the respective peaks observed at 1061 cm^{-1} and 1024 cm^{-1} which is also corroborated with the PXRD data (*vide infra*).[67b] Similar trend was also observed for cellulose NP crystalline arrangement and amorphous character observed at 1080 cm^{-1} and 1022 cm^{-1}, respectively.

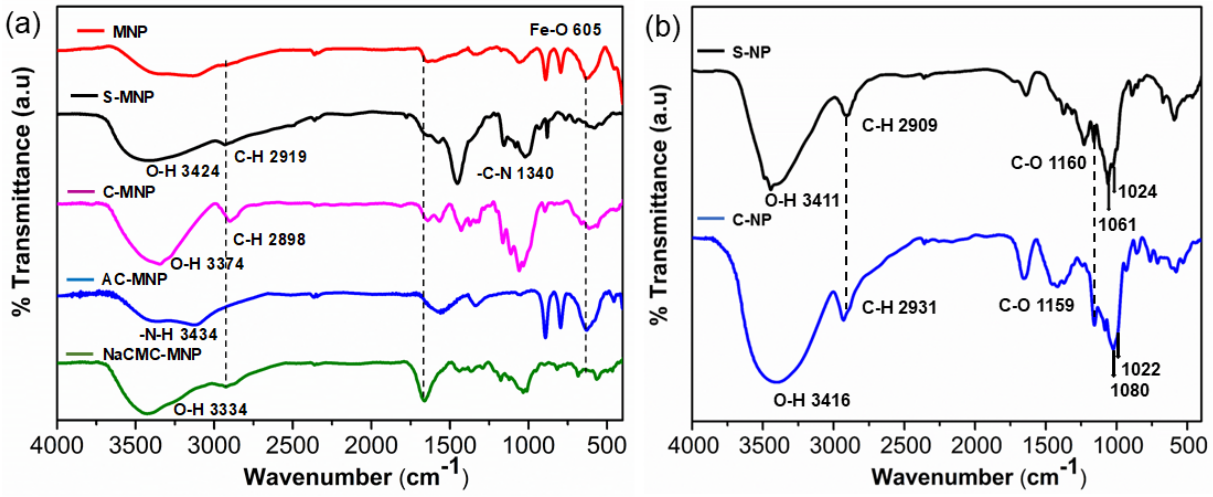

Figure 3. FT-IR spectra of the synthesized nanocomposites: (a) Hybrid-NCs, (b) organic-NCs.

3.2.2 PXRD analysis. Powder XRD (PXRD) pattern of MNP (Fe_3O_4 NPs), hybrid- and organic-NCs are shown in Figure 4 (a, b). The PXRD pattern of MNP showed the diffraction peaks at

30.0°, 35.6°, 43.3°, 53.3°, 57.3°, and 62.8° corresponds to (111), (220), (311), (400), (422), and (511) planes of magnetite that matches with the JCPDS no. 03–0863.[67,70,71,73] Comparative PXRD pattern analysis of S-MNP, and C-MNP showed the presence of characteristic peaks for MNP, which suggests the binding of magnetite NP. In contrast, the AC-MNP and NaCMC-MNP have not shown sharp peaks indicating amorphous nature.[67a,71-74] The crystallite size of the pure MNP sample and the MNP nanocomposites was determined based on the Scherrer equation using the prominent characteristic peaks position at 2θ = 35.6°. Accordingly, the average crystallite sizes of various samples viz., MNP, S-MNP, and C-MNP were 9.80, 10.87, and 11 nm, respectively, as calculated by the Debye-Scherrer equation. Organic NCs, S-NP showed clear peaks due to more ordered amylopectin content, while the C-NP has shown amorphous nature.

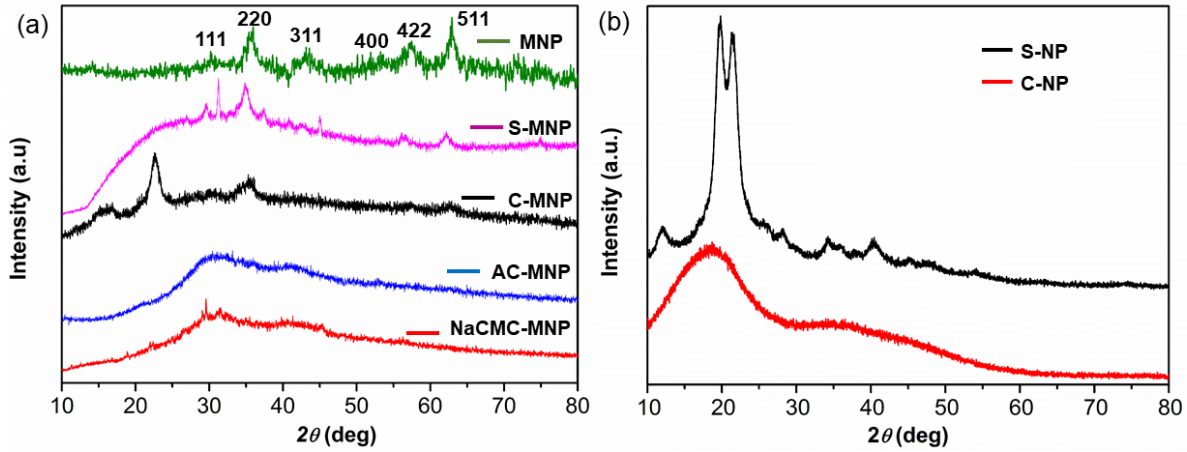

Figure 4. PXRD pattern for a) hybrid nanocarriers, b) organic nanocarriers.

3.2.3 Particles size analysis and surface Morphology by TEM, AFM & SEM studies. The control of the monodispersed smaller-sized NP is essential because nanocrystal properties strongly depend upon the surface area of the NP. The TEM images and histograms of NCs are provided in Figures 5 and S1, respectively, and all of them exhibited smaller sizes of <50 nm. To the best of our knowledge, such a smaller NP for the pesticide delivery application has not been reported (Table S4, SI). More accurately, the hybrid NCs such as S-MNP, C-MNP, AC-MNP, and NaCMC-MNP have exhibited an average diameter of 6, 8, 23, and 8 nm, respectively (Figure S1, SI). The morphology of hybrid-NCs revealed that the samples composed of highly distributed NP with a spherical shape except for the AC-MNP showed the clusters of aminocellulose coated MNP with the mean size of 23 nm (Figure 5c). The presence of polysaccharides such as starch prevents the agglomeration of the MNP and this stability remains even after 6 months. This means that starch chains wrapping around the MNP *via* the

interaction between the hydroxyl group and iron provide high colloidal stability. HR-TEM images of all hybrid NCs have shown an individual MNP with a lattice spacing of 0.3 nm corresponds to the *d* spacing of the cubic plane of MNP (Figure S2).

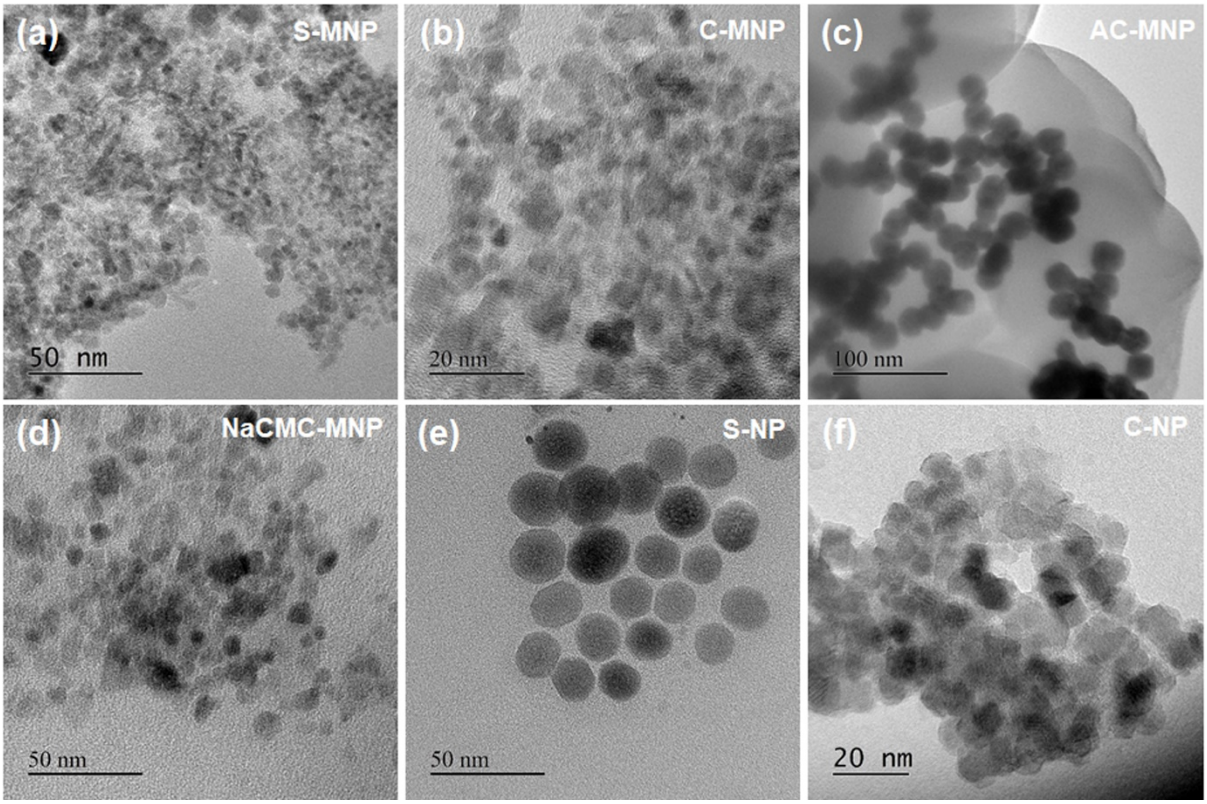

Figure 5. TEM images for (a) S-MNP (b) C-MNP (c) AC-MNP (d) NaCMC-MNP (e) S-NP (f) C-NP.

The particles size on TEM micrographs of organic NCs *viz.,* S-NP and C-NP was observed ~ 20 and 18 nm, respectively (Figures 5e and 5f). Starch has shown spherical, monodisperse NP with no aggregation, while cellulose showed irregular spheres aggregated nanoparticles probably due to strong hydrogen bonding established between the cellulose NP.[75,76]

To shed more light on the surface morphology of the hybrid- and organic-NCs, the AFM and SEM images were recorded and presented in Figures S4 and S5. The AFM image of S-MNP revealed that the highly dispersed spherical MNP were formed (Figure S4a). In the case of C-MNP (Figure S4b), irregular spheres dispersed in the cellulose matrix as observed in the TEM. In Figure S4c, the AC-MNP showed clearly the incorporation of MNP in the aminocellulose matrix. It is also possible to note a significant level of agglomeration. NaCMC-MNP particles have been found to exhibit homogeneously dispersed. While the organic nanocarriers S-NP

and C-NP showed the relevant smooth and good structural integrity (Figures S4e,f). The SEM images (Figure S5) of hybrid nanocomposites were also in corroboration with the morphology observed in AFM images. The digital photographs of all NCs are shown in Figure S6.

3.2.4 Vibrating sample magnetometer (VSM). The magnetic characteristics of the prepared hybrid MNP NCs were measured using VSM in the presence of a magnetic field. The magnetic stability of hybrid MNP comparing hysteresis loops at 5 K and 300 K is given in Figure 6.

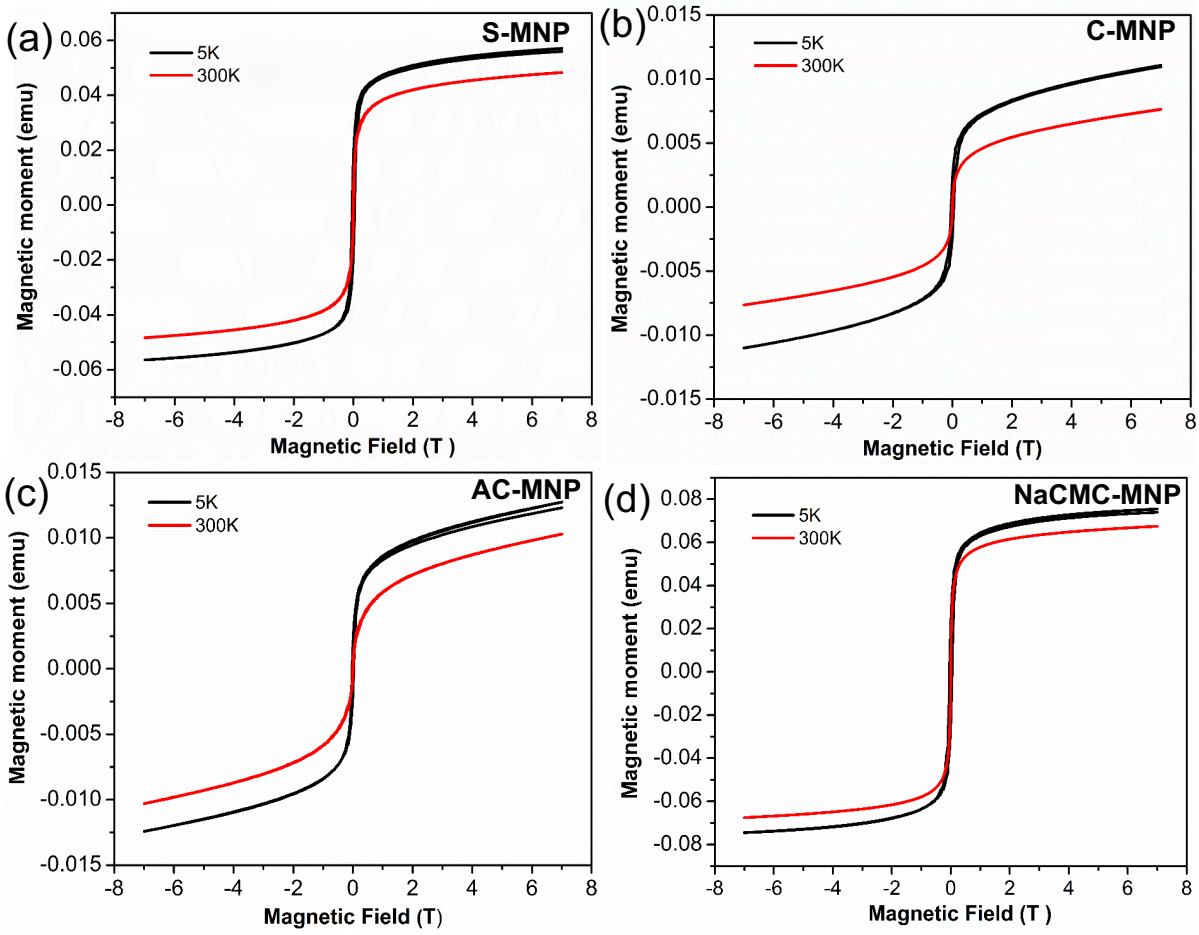

Figure 6. Magnetic hysteresis curves for the as-synthesized: (a) S-MNP, (b) C-MNP, (c) AC-MNP, and (d) NaCMC-MNP.

The VSM comparison study of hybrid MNPs results illustrated that the magnetic moment of S-MNP and NaCMC-MNP composites appears maximum. In contrast, C-MNP and AC-MNP could not achieve their saturation magnetization (Figure 6). All hybrid MNPs are found to exhibit ferromagnetic character. The VSM results affirm that NaCMC-MNP and S-MNP have good magnetic properties, as well as magnetic stability. These results suggest that NaCMC-

MNP and S-MNP may be helpful in the recovery of the used NCs using an external magnet and can be considered one of the potential biomaterials in field applications.

3.2.5 TGA Analysis. The TGA analysis was performed to determine the organic content of the hydrophilic polymer attached to MNP (Figure S7). The measurement was carried out under N_2 atmosphere from 30 °C to 1000 °C, with a heating rate of 10 °C/min. In Figure S7a, all hybrid NCs have shown a small weight loss of 8–11% till 210 °C, ascribed to the release of moisture from the samples. Hybrid-NCs such as C-MNP, AC-MNP, and NaCMC-MNP have shown single-stage steady decomposition from 210 to ~600 °C with weight losses of 8, 46, and 38%, respectively. In the case of S-MNP, the decomposition occurs at clearly two stages, one at 283 °C followed by 619 °C with weight loss up to 17% at 960 °C, indicating a more stable nanocarrier than cellulose, as the latter has shown complete degradation with the lowest temperature of 490 °C. We infer that the two-stage degradation of starch may correspond to the presence of amylopectin and amylose structures in starch.

The TGA profiles of organic NCs, S-NP and C-NP are shown in Figure S7b. Similar to hybrid NCs, here too, the starch NP has shown two stages of decomposition at 360 °C and 415 °C corroborating the presence of amylopectin and amylose degradation in starch. Unlike in MNP, the cellulose has shown two steps degradations, one at 181 °C to about 64% and complete degradation at 489 °C. Interestingly, the comparative evaluation of the thermal profiles of S-MNP and S-NP showed that the temperature for onset of thermal degradation was much lower for S-NP (~490 °C) than the nanocomposite S-MNP indicating the hybrid NCs exhibit excellent thermal stability over organic NCs.

3.3 Comparison of PLE wt% and E.E % for organic- and hybrid-NCs.

Pesticide loading efficiency (PLE, wt%) and encapsulation efficiency (E.E %) were quantified using gas chromatography−mass spectrometry (GC-MS) analysis after the successful loading of chlorpyrifos (ChP) pesticide onto the hybrid- and organic-NCs (Table 1, Tables S2 and S3 in SI). However, the pesticide is expected to be entrapped within pores of the cavities generated due to the entanglement of polysaccharide chains. It is imperative to quantify and adjust the inorganic content present in hybrid NCs as MNP for a fair comparison to organic NCs using ICP-MS (for details, see Section B, SI). The corrected E.E % and PLE wt% values were listed in Table 1.

Table 1. Comparison of E.E% and PLE wt% of hybrid- and organic-NCs

[a] E.E % and PLE wt% obtained from GC-MS (Table S2) including MNP part, [b] in case of hybrid-NCs correction was applied by replacing the inorganic content to organic using ICP-MS (the calculation is provided in Section B3, ESI. [c] Relative PLE wt% with respect to S-MNP = corrected PLE of (other MNP / S-MNP)*100.

Types of NC	NC	E.E (%)[a]	PLE (%)[a]	Corrected E.E(%)[b]	Corrected PLE (wt %)[b]	Relative PLE(wt %) [c]
Hybrid	S-MNP	20.7	93.3	24.6	111	100
	C-MNP	16.7	75.2	19.0	86	77
	AC-MNP	16.4	73.8	17.8	80	73
	NaCMC-MNP	16.9	76.0	20.9	94	85
organic	S-NP	19.3	87.0	19.3	87	79
	C-NP	18.0	81.0	18.0	81	73

Overall, almost all the NCs have shown efficient entrapment of ChP into polysaccharide NP with the corrected E.E % and PLE wt% values ranging between 17.8–24.6% and 81–111 wt%, respectively. Comparison of corrected PLE wt% values have revealed a couple of observations, i) hybrid-NCs S-MNP (111 wt%) and C-MNP (86 wt%) showed significantly better performance than corresponding organic-NCs S-NP (87 wt%) and C-NP (81 wt%), respectively. This is particularly true for S-MNP, which has shown remarkably high PLE wt%. ii) Among the cellulose-based NCs, amine-functionalized AC-MNP exhibited less PLE wt% of 80 wt% than the COONa functionalization in NaCMC-MNP, which showed ~94 wt% while unfunctionalized cellulose showed 86%. These results indicate that though slight alternation was found in terms of PLE wt%, functionalization did not significantly improve the PLE wt% value. iii) Among the hybrid-NCs, S-MNP has outperformed over cellulose derivatives. Based on these results, we infer that the high performance of starch over cellulose derivatives may be attributed to the branching nature of starch due to β-1,4- & 1,6-linkages of glucose unit upon binding on the MNP can generate more rooms for the loading of the pesticide.

3.4 In-vitro aqueous release behaviour of nanocarriers. Time-dependent pesticide release behaviour was determined based on the absorbance of ChP monitored using UV–Vis spectroscopy. Figures 7a and 7b show the release profiles of hybrid- and organic-NCs, respectively. Initial pH for all NCs was recorded in an aqueous medium and the results are shown in Table S5, SI. Among the hybrid-NCs, the AC-MNP and NaCMC-MNP have shown inferior release profiles of 24 and 20 %, respectively, in 4 days which did not improve even up

to 17 days. Then, C-MNP has shown an initial burst release of 49 % in two days followed by a sustained release up to 61 % in 13 days, which did not improve even up to 17 days. The inferior release profiles for the carboxylate (NaCMC-MNP) and amine (AC-MNP) functionalized celluloses might be due to functional groups such as pyridine and phosphate ester present in the ChP, which can have relatively stronger interactions (non-covalent interactions, for instance, ionic (electrostatic), H-bonding, *etc.*) with charged celluloses. In contrast, neutral cellulose that contains no charged functional groups may have weaker interactions with pesticide molecules, thus allowing the release faster. Interestingly, S-MNP has shown a better release profile with an initial burst release of 44 % in one day followed by a remarkable steady release of 89 % for up to 10 days which did not improve up to 17 days. These results imply that overall, the cellulose-based polysaccharides have shown inferior release profiles than starch, presumably due to the branched nature, which creates bigger rooms while holding on to the MNP support. The better C-NP vs. C-MNP also supports this. To verify the role of surface morphology and its contribution in the increased E.E % and PLE wt% for starch was investigated using the SEM images. The morphology profile indicates that starch show significantly different fine texture suggesting the better pesticide adsorption (Figure S4a and b). Further comparison of release profiles within the cellulose-based NCs indicates that chemical modification does not give healthier aqueous release results. However, in contrast to C-MNP, organic C-NP has shown a better and steady release profile having an initial burst release of 52 % in two days followed by a controlled release of 76 % for up to 8 days. However, S-NP has shown a similar release profile to hybrid S-MNP, having an initial burst release of 42 % in one day followed by a steady release of 82 % in 8 days. After 8 days, no significant increase was observed for up to 17 days. These results suggest that starch is outperforming in both organic and hybrid systems concerning loading and SPR %. The observation of initial burst followed by steady release has been considered advantageous. It will be readily available to kill the existing pest and subsequently kill and inhibit new infestation.

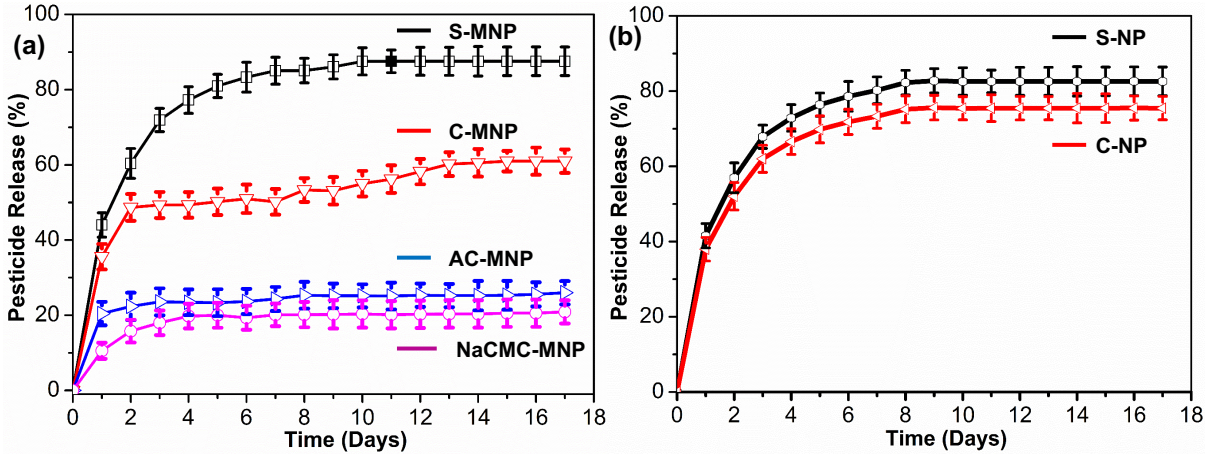

Figure 7. Aqueous release behaviour of ChP for a) hybrid- and b) organic-NCs.

Release kinetics. Only Makoid–Banakar Model to the following empirical equation 3 showed the goodness of fit based on (Figure S9), the correlation coefficient (R^2), the adjusted coefficient of determination (R^2_adj), the sum of squares of residues (SSR), the mean square error (MSE), the Akaike Information Criterion (AIC), and MSC values (Table S6).[69,77] On the other hand, release kinetics fitting with Korsmeyer–Peppas and Peppas–Sahlin model are shown in (Figure S10 and S11) respectively and the R^2 and R^2_adj values are given in Table S7.

$$F = M_t/M_0 = kMB\ t^n \exp^{-ct} \quad (3)$$

where M_t/M_0 is the percentage of ChP released at time t, and kMB, n, and c are empirical parameters (kMB, n, c > 0). F-ratio probability is commonly used as a pesticide-release model selection criterion. The R^2 adjusted value was used as the model selection criterion with the best fit model showing in Table S6. the R^2 adjusted value closest to 1.[77,78]

Table 2. Best-fit values and secondary parameters from the fitting Makoid-Banakar model.

Type of NCs	**NCs**	**Parameter**			
		kMB	**n**	**k**	**T25**
Hybrid-NCs	S-MNP	58.487	0.267	0.023	1.622
	C-MNP	46.609	0.008	0.017	1.722
	AC-MNP	22.091	0.005	0.014	7.235

	NaCMC-MNP	16.557	0.152	0.013	-
Organic-NCs	S-NP	55.638	0.286	0.026	1.698
	C-NP	50.841	0.286	0.026	1.721

The parameter k of the Makoid–Banakar model did not equal zero for all the NCs. Further, the T25 value increase from C-MNP to NaCMC-MNP as given in Table 2, which indicates the pesticide release deceleration from C-MNP to NaCMC-MNP. In Table 2, the parameter of n values from the Makoid–Banakar model were not close to ∼0.43. Thus the mechanism of pesticide release from both hybrid and organic NCs is a significant effect of the diffusion principle.[79] The formation of a porous structure in the S-MNP on swelling in water is expected to enhance the release. This results in the release of ChP being controlled by diffusion through the polysaccharides rather than by the swelling of polysaccharides.

4. CONCLUSIONS

We systematically designed, synthesized, and characterized the hybrid- and organic-NCs with various polysaccharides to discern the role of inorganic support used in the hybrid-NCs and the type of nanomaterials synthesis such as hybrid *vs.* organic systems being adopted for pesticide delivery. Further, to understand the beneficial effect of functionalization of natural polysaccharide (cellulose), this study has unravelled the answers to these questions. Though MNP support does not exhibit many benefits for the cellulose derivatives (PLE: 80 – 94 wt%, SPR: 60-20 %), the starch has shown outstanding PLE (111 wt%) and SPR (87 % in 10 in days) results. The superior performance (SPR %) of starch might be due to the β-1,4- and 1,6-linkages of sugar moieties absent in cellulose derivatives leading to the branched polymers onto the MNP support. This brings more room for the pesticides to be entrapped and allows them to release sustainably.

Further, the results infer that the functionalization of cellulose derivatives is not beneficial. Though S-MNP showed a better PLE wt% and similar SPR % profile compared to organic S-NC, by keeping the cost and benefits balance, the organic-NCs are better for practical use as pesticide delivery agents. It is noteworthy that unlike previously reported polysaccharide nanocomposites-based NCs, the present NCs have shown good to excellent PLE (81-111 wt%) owing to their smaller-sized particles. We believe that the lessons learned in this study would

help researchers working in the pesticide delivery for designing and improving the NCs to achieve practical agricultural applications.

ASSOCIATED CONTENTS

Supplementary Information.

The Supporting Information (SI) is available free of charge. Elemental composition study by TEM–EDX, AFM, SEM, and pH measurements data, calculations details of PLE wt% and E. E% estimation, and a comparison table with literature NC system.

AUTHOR INFORMATION

Corresponding Author

*(G.J.) E-mail: jayamurugan@inst.ac.in

ORCID

Ritu Mahajan: 0000-0001-5590-3539

Abdul Selim: 0000-0002-6441-411X

K. M. Neethu: 0000-0002-2686-3731

Sandeep Sharma: 0000-0002-7465-5208

Vijayakumar Shanmugam: 0000-0001-7117-5631

Govindasamy Jayamurugan: 0000-0001-9870-5209

Author Contributions

† These authors contributed equally. The manuscript was written through the contributions of all authors. All authors have approved the final version of the manuscript.

Notes

The authors declare no competing financial interest.

ACKNOWLEDGMENTS

This work was supported by the SERB, Department of Science and Technology (DST), Grant Nos. SB/S2/RJN-047/2015 and SR/WOS-B/818/2016 (G) and Department of Biotechnology (DBT), Grant No BT/CIAB-Flagship/2018. GJ and RM thank DST-SERB for Ramanujan and WOS-B Fellowships, respectively. The authors thank Punjab Biotechnology Incubator for ICP-MS measurements.

REFERENCES

(1) McClung C R 2014 Making Hunger Yield *Science* **344** 699.

(2) Medina-Pérez G et al. 2019 Nanotechnology in crop protection: Status and future trends. In Koul O (ed) Nano-Biopesticides Today and Future Perspectives. Academic Press, pp. 17–45.

(3) Popp J, Pető K and Nagy J 2013 Pesticide productivity and food security. A review. *Agron. Sustain. Dev.* **33** 243.

(4) Jia H 2019 Agriculture: science and technology safeguard sustainability *Natl. Sci. Rev.* **6** 595.

(5) Singh A et al. 2019 Advances in Controlled Release Pesticide Formulations: Prospects to Safer Integrated Pest Management and Sustainable Agriculture *J. Hazard. Mater.* **385**, 121525.

(6) Nuruzzaman M et al. 2019 Nanobiopesticides: composition and preparation methods. In Koul O (ed) Nano-Biopesticides Today and Future Perspectives. Academic Press pp. 69–131.

(7) Kah M, Beulke S, Tiede K and Hofmann T 2013 Nanopesticides: State of Knowledge, Environmental Fate, and Exposure Modeling. *Crit. Rev. Environ. Sci. Technol.* **43** 1823.

(8) (a) Zhao X et al. 2018 Development Strategies and Prospects of Nano-based Smart Pesticide Formulation *J. Agric. Food Chem.* **66** 6504. (b) Tong Y et al. 2017 Polymeric Nanoparticles as a Metolachlor Carrier: Water-Based Formulation for Hydrophobic Pesticides and Absorption by Plants *J. Agric. Food Chem.* **65** 7371.

(9) (a) Khot L R et al. 2012 Applications of nanomaterials in agricultural production and crop protection *Crop Prot.* **35** 64. (b) Gogos A, Knauer K and Bucheli T D 2012 Nanomaterials in Plant Protection and Fertilization: Current State, Foreseen Applications, and Research Priorities *J. Agric. Food Chem*. **60** 9781.

(10) Huang B et al. 2018 Advances in Targeted Pesticides with Environmentally Responsive Controlled Release by Nanotechnology *Nanomaterials* **8** 102.

(11) Singh R P 2017 Application of Nanomaterials Toward Development of Nanobiosensors and Their Utility in Agriculture. In: Prasad R, Kumar M and Kumar V (eds) Nanotechnology. Springer (Singapore). pp 293.

(12) Singhal N K, Singh V and Kaushal S 2018 Applications of Nanoagrochemicals Precepts and Prospects. In Singh B, Katare O P and Souto E B (eds) NanoAgroceuticals & NanoPhytoChemicals. CRC Press. (Boca Raton), pp 13.

(13) Damalas C A and Koutroubas S D 2016 Farmers Exposure to Pesticides: Toxicity Types and Ways of Prevention *Toxics* **4** 1.

(14) De A, Bose R, Kumar A and Mozumdar S 2014 Targeted Delivery of Pesticides Using Biodegradable Polymeric Nanoparticles. In De A, Bose R, Kumar A and Mozumdar S (eds) Introduction. Springer (New Delhi), pp. 1–4.

(15) Chi Y, Zhang G, Xiang Y, Cai D and Wu Z 2017 Fabrication of a Temperature-Controlled-Release Herbicide Using a Nanocomposite *ACS Sustain. Chem. Eng.* **5** 4969.

(16) Gerstl Z, Nasser A and Mingelgrin U 1998 Controlled Release of Pesticides into Soils from Clay−Polymer Formulations *J. Agric. Food Chem.* **46** 3797.

(17) Xiang S et al. 2019 Dual-Action Pesticide Carrier That Continuously Induces Plant Resistance, Enhances Plant Anti-Tobacco Mosaic Virus Activity, and Promotes Plant Growth *J. Agric. Food Chem.* **67** 10000.

(18) Alonso-Díaz A et al. 2019 Enhancing Localized Pesticide Action through Plant Foliage by Silver-Cellulose Hybrid Patches *ACS Biomater. Sci. Eng.* **5** 413.

(19) Zhong B et al. 2017 Halloysite Tubes as Nanocontainers for Herbicide and Its Controlled Release in Biodegradable Poly(vinyl alcohol)/Starch Film *J. Agric. Food Chem.* **65** 10445.

(20) Nuruzzaman M, Rahman M M, Liu Y and Naidu R 2016 Nanoencapsulation, Nano-guard for Pesticides: A New Window for Safe Application *J. Agric. Food Chem.* **64** 1447.

(21) Ayoub H A, Khairy M, Elsaid S, Rashwan F A and Abdel-Hafez H F 2018 Pesticidal Activity of Nanostructured Metal Oxides for Generation of Alternative Pesticide Formulations *J. Agric. Food Chem.* **66** 5491.

(22) Balas M et al. 2017 Synthesis, Characterization, and Toxicity Evaluation of Dextran-Coated Iron Oxide Nanoparticles *Metals* **7** 63.

(23) Sharma L and Kakkar R 2017 Hierarchical Porous Magnesium Oxide (Hr-MgO) Microspheres for Adsorption of an Organophosphate Pesticide: Kinetics, Isotherm, Thermodynamics, and DFT Studies *ACS Appl. Mater. Interfaces* **9** 38629.

(24) Chen H et al. 2016 Synthesis and Characterization of Chlorpyrifos/Copper(II) Schiff Base Mesoporous Silica with pH Sensitivity for Pesticide Sustained Release *J. Agric. Food Chem.* **64** 8095.

(25) Wang Y, Cui H, Sun C, Zhao X and Cui B 2014 Construction and evaluation of controlled-release delivery system of Abamectin using porous silica nanoparticles as carriers *Nanoscale Res. Lett.* **9** 655.

(26) Cao L, Zhang H, Cao C, Zhang J, Li F and Huang Q 2016 Quaternized Chitosan-Capped Mesoporous Silica Nanoparticles as Nanocarriers for Controlled Pesticide Release *Nanomaterials* **6** 126.

(27) Gerstl Z, Nasser A and Mingelgrin U 2011 Slow-Release Formulation of a New Biological Pesticide, Pyoluteorin, with Mesoporous Silica *J. Agric. Food Chem.* **59** 307.

(28) Nuruzzaman M et al. 2020 Hollow Porous Silica Nanosphere with Single Large Pore Opening for Pesticide Loading and Delivery *ACS Appl. Nano Mater.* **3**, 105.

(29) Maliyekkal S M et al. 2013 Graphene: A Reusable Substrate for Unprecedented Adsorption of Pesticides *Small* **9** 273.

(30) Sharma S, Singh S, Ganguli A K and Shanmugam V 2017 Anti-drift nano-stickers made of graphene oxide for targeted pesticide delivery and crop pest control *Carbon* **115** 781.

(31) Liu Z et al. 2016 Fe_3O_4@Graphene Oxide@Ag Particles for Surface Magnet Solid-Phase Extraction Surface-Enhanced Raman Scattering (SMSPE-SERS): From Sample Pretreatment to Detection All-in-One *ACS Appl. Mater. Interfaces* **8** 14160.

(32) Pinto R C, Neufeld R J, Ribeiro A J and Veiga F 2006 Nanoencapsulation I Methods for Preparation of Drug Loaded Polymeric Nanoparticles *Nanomed. Nanotechnol. Biol. Med.* **2** 8.

(33) Roy A, Bajpai J and Bajpai A K 2009 Dynamics of controlled release of chlorpyrifos from swelling and eroding biopolymeric microspheres of calcium alginate and starch *Carbohydr. Polym*. **76** 222.

(34) Matricardi P, Di Meo C, Coviello T, Hennink W E and Alhaique F 2013 Interpenetrating polymer networks polysaccharide hydrogels for drug delivery and tissue engineering *Adv. Drug Deliv. Rev.* **65** 1172.

(35) Khan F, Tanaka M and Ahmad S R Fabrication of polymeric biomaterials: a strategy for tissue engineering and medical devices *J. Mater. Chem. B.* **3** 8224.

(36) Neri-Badanga M C and Chakrabortya S 2019 Carbohydrate polymers as controlled release devices for pesticides *J. Carbohydr. Chem*. **38** 67.

(37) Campos E V R, Oliveira J L D, Fraceto L F and Singh B 2015 Polysaccharides as safer release systems for agrochemicals *Agron. Sustain. Dev.* **35** 47.

(38) Luo Y and Wang Q 2014 Recent development of chitosan-based polyelectrolyte complexes with natural polysaccharides for drug delivery *Int. J. Biol. Macromol.* **64** 353.

(39) Xu X, Bai B, Wang H and Suo Y 2017 A Near-Infrared and Temperature-Responsive Pesticide Release Platform through Core−Shell Polydopamine@PNIPAm Nanocomposites *ACS Appl. Mater. Interfaces* **9** 6424.

(40) Hao L et al. 2019 Phosphorylated Zein as Biodegradable and Aqueous Nanocarriers for Pesticides with Sustained-Release and anti-UV Properties *J. Agric. Food Chem.* **67** 9989.

(41) Madhusudhan R A, Karthikeyan R, Vejandla R S, Divya G and Babu P S 2017 Controlled release matrix drug delivery system – a review *Int. J. Allied Med. Sci. Clin. Res.* **5** 384.

(42) Bhattarai N, Gunn J and Zhang M 2010 Chitosan-based hydrogels for controlled, localized drug delivery *Adv. Drug Deliv. Rev.* **62** 83.

(43) Giri T K, Thakur A, Alexander A, Badwaik H and Tripathi D K 2012 Modified chitosan hydrogels as drug delivery and tissue engineering systems: present status and applications *Acta Pharm. Sin. B* **2** 439.

(44) Shafiee A and Atala A 2017 Tissue engineering: toward a new era of medicine *Annu. Rev. Med*. **68** 29.

(45) Martins A M et al. 2014 Electrically conductive chitosan/carbon scaffolds for cardiac tissue engineering *Biomacromolecules* **15** 635.

(46) Seweryn A and Bujak T 2018 Application of Anionic Phosphorus Derivatives of Alkyl Polyglucosides for the Production of Sustainable and Mild Body Wash Cosmetics *ACS Sustainable Chem. Eng.* **6** 17294.

(47) Adisa I O et al. 2019 Recent advances in nano-enabled fertilizers and pesticides: a critical review of mechanisms of action *Environ. Sci.: Nano* **6** 2002.

(48) Nair R et al. 2010 Nanoparticulate Material Delivery to Plants *Plant Sci.* **179** 154.

(49) Rajakumar R and Sankar J 2016 Hydrogel: novel soil conditioner and safer delivery vehicle for fertilizers and agrochemicals – a review *Int. J. Appl. Pure Sci. Agric.* **2** 163.

(50) Grillo R et al. 2014 Chitosan/tripolyphosphate nanoparticles loaded with paraquat herbicide: An environmentally safer alternative for weed control *J. Hazard. Mater.* **278**, 163.

(51) DeLoid G M et al. 2018 Reducing Intestinal Digestion and Absorption of Fat Using a Nature-Derived Biopolymer: Interference of Triglyceride Hydrolysis by Nanocellulose *ACS Nano* **12** 6469.

(52) Singh B, Sharma D K, Kumar R and Gupta A 2009 Controlled release of the fungicide thiram from starch–alginate–clay based formulation *Appl. Clay Sci.* **45**, 76.

(53) Fernández-Pérez M, Villafranca-Sánchez M, González-Pradas E, Martinez-López F and Flores-Céspedes F 2000 Controlled Release of Carbofuran from an

626 Alginate−Bentonite Formulation: Water Release Kinetics and Soil Mobility *J. Agric.*
627 *Food Chem.* **48** 938.
628 (54) Garrido-Herrera F J, González-Pradas E and Fernández-Pérez M 2006 Controlled
629 Release of Isoproturon, Imidacloprid, and Cyromazine from Alginate−Bentonite-
630 Activated Carbon Formulations *J. Agric. Food Chem.* **54** 10053.
631 (55) Flores-Céspedes F, Pérez-García S, Villafranca-Sánchez M and Fernández-Pérez M
632 2013 Bentonite and anthracite in alginate-based controlled release formulations to
633 reduce leaching of chloridazon and metribuzin in a calcareous soil *Chemosphere* **92** 918.
634 (56) Silva M d S et al. 2011 Paraquat-loaded alginate/chitosan nanoparticles: preparation,
635 characterization and soil sorption studies *J. Hazard. Mater,* **190** 366.
636 (57) Işiklan N 2007 Controlled release study of carbaryl insecticide from calcium alginate
637 and nickel alginate hydrogel beads *J. Appl. Polym. Sci.***105** 718.
638 (58) Kumbar S G, Kulkarni A R, Dave A M and Aminabhavi T M 2001 Encapsulation
639 efficiency and release kinetics of solid and liquid pesticides through urea formaldehyde
640 crosslinked starch, guar gum, and starch + guar gum matrices *J. Appl. Polym. Sci.* **82**
641 2863.
642 (59) Fátima Sopeña, Alegría Cabrera, Celia Maqueda and Esmeralda Morillo 2005
643 Controlled Release of the Herbicide Norflurazon into Water from Ethylcellulose
644 Formulations *J. Agric. Food Chem.* **53** 3540.
645 (60) Sopeña F, Cabrera A, Maqueda C and Morillo E 2007 Ethylcellulose Formulations for
646 Controlled Release of the Herbicide Alachlor in a Sandy Soil *J. Agric. Food Chem.* **55**
647 8200.
648 (61) Flores-Céspedes F, Daza-Fernández I, Villafranca-Sánchez M and Fernández -Pérez
649 M 2009 Use of Ethylcellulose To Control Chlorsulfuron Leaching in a Calcareous Soil
650 *J. Agric. Food Chem.* **57** 2856.
651 (62) Fernández-Pérez M, Villafranca-Sánchez M, Flores-Céspedes F and Daza-Fernández
652 I 2011 Ethylcellulose and lignin as bearer polymers in controlled release formulations
653 of chloridazon *Carbohyd. Polym.* **83** 1672.
654 (63) Li J, Yao J, Li Y and Shao Y 2012 Controlled release and retarded leaching of pesticides
655 by encapsulating in carboxymethyl chitosan/bentonite composite gel *J. Environ. Sci*
656 *Health B*. **47** 795.
657 (64) He F et al. 2019 Fabrication of a sustained release delivery system for pesticides using
658 interpenetrating polyacrylamide/alginate/montmorillonite nanocomposite hydrogels
659 *Appl. Clay Sci.* **183** 105347.

660 (65) Riyajan S –A and Sakdapipanich J T 2009 Development of a controlled release neem
661 capsule with a sodium alginate matrix, crosslinked by glutaraldehyde and coated with
662 natural rubber *Polym. Bull.* **63** 609.
663 (66) Kulkarni A R et al. 1999 Urea-formaldehyde crosslinked starch and guar gum matrices
664 for encapsulation of natural liquid pesticide [Azadirachta Indica A. Juss. (neem) seed
665 oil]: swelling and release kinetics *J. Appl. Polym. Sci.* **73** 2437.
666 (67) (a) Gupta A et al. 2018 Nanocarrier composed of magnetite core coated with three
667 polymeric shells mediates LCS-1 delivery for synthetic lethal therapy of BLM-defective
668 colorectal cancer cells *Biomacromolecules* **19** 803. (b) Liu T Y, Ma Y, Yu S F, Shi J and
669 Xue S 2011 The effect of ball milling treatment on structure and porosity of maize starch
670 granule *Innov. Food Sci. Emerg. Technol*. **12** 586. (c) Hossein H H S et al. 2020
671 Functionalization of Magnetic Nanoparticles by Folate as Potential MRI Contrast Agent
672 for Breast Cancer Diagnostics *Molecules* **25** 4053.
673 (68) (a) Ritger P L and Peppas N A 1987 A simple equation for description of solute release
674 I. Fickian and anomalous release from nonswellable devices in the form of slabs,
675 spheres, cylinders or discs *J. Control. Release* **5** 23. (b) Peppas N A and Sahlin J J 1989
676 A simple equation for the description of solute release. III. Coupling of diffusion and
677 relaxation *Int. J. Pharm*. **57** 169.
678 (69) Makoid M C, Dufoure A and Banakar U V 1993 Modelling of dissolution behaviour of
679 controlled release systems *STP Pharma Prat*. **3** 49.
680 (70) Zhang J, Elder T J, Pu Y and Ragauskas A J 2007 Facile synthesis of spherical cellulose
681 nanoparticles *Carbohydr. Polym.* **69** 607.
682 (71) Sadeghi R, Daniella Z, Uzun S and Kokini J 2017 Effects of starch composition and
683 type of non-solvent on the formation of starch nanoparticles and improvement of
684 curcumin stability in aqueous media *J. Cereal Sci.* **76** 122.
685 (72) Dung T T, Danh T M, Hoa L T M, Chien D M and Duc N H 2009 Structural and
686 magnetic properties of starch-coated magnetite nanoparticles *J. Exp. Nanosci.* **4** 259.
687 (73) Ayala-Valenzuela O et al. 2005 Magnetite-cobalt ferrite nanoparticles for
688 kerosenebased magnetic fluids *J. Magn. Magn. Mater*. **294** e37.
689 (74) Kaur S et al. 2020 Tuning of the Cross-Glaser Products mediated by Substrate-
690 Catalyst's Polymeric Backbone Interactions *Chem. Commun*. **56** 2582.
691 (75) Yu X et al. 2013 One-step synthesis of magnetic composites of cellulose@iron oxide
692 nanoparticles for arsenic removal *J. Mater. Chem. A* **1**, 959.

(76) Laurent S et al. 2008 Magnetic Iron Oxide Nanoparticles: Synthesis, Stabilization, Vectorization, Physicochemical Characterizations, and Biological Applications *Chem. Rev*. **108** 2064.

(77) Costa P and Sousa Lobo J M 2001 Modeling and comparison of dissolution profiles *Eur. J. Pharm. Sci.* **13** 123.

(78) Catalan-Figueroa J et al. 2018 A mechanistic approach for the optimization of loperamide loaded nanocarriers characterization: Diafiltration and mathematical modeling advantages *Eur. J. Pharm. Sci.* **125** 215.

(79) Ilango K B and Kavaimani S 2015 In vitro evaluation and mechanism of drug release from natural mucilage-based colon-site specific drug delivery system *Int. J. Pharm Tech Res.* **7** 185.

Table of Contents

A Systematic Study to Unravel the Potential of using Polysaccharides based Organic Nanoparticles Versus Hybrid Nanoparticles for Pesticide Delivery

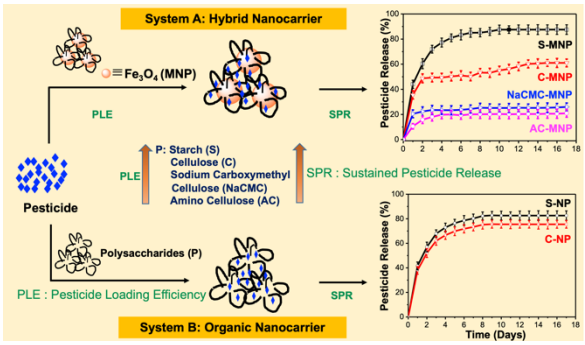

Hybrid *vs* organic nanocarriers were compared for pesticide encapsulation and release behavior. Among the polysaccharides, the MNP support was beneficial for starch. In general, the present NCs have shown good results owing to their smaller-sized particles.